

# Novel transflective liquid crystal displays having a single cell gap and a single LC mode combined with an inner-patterned retarder

*Sin-Doo Lee\**, *Yong-Woon Lim*, *Jinyool Kim*, and *Dong-Woo Kim*

School of Electrical Engineering #32, Seoul National University, Kwanak P.O.Box 34,  
Seoul 151-600, Korea

Phone: +82-2-872-8643, E-mail: sidlee@plaza.snu.ac.kr

## Abstract

We report on new transflective liquid crystal displays (LCDs) having a single cell gap and a single LC mode combined with an inner-patterned retarder. In a vertically or planarly aligned configuration the brightness is greatly improved and a single driving scheme can be employed.

## 1. Introduction

Transflective liquid crystal displays (LCDs) will become significant for mobile applications because of their low power consumption and outdoor readability [1, 2]. The transflective LCDs are normally divided into the transmissive and reflective regions. A typical way of compensating the optical path difference between the two regions is to use a multi-gap design [2, 3]. However, such multi-gap design involves complicated fabrication processes and results in low production yield. In order to overcome these problems, a single gap design having periodically patterned electrodes [4] or two different modes in subpixels [5] has been recently demonstrated. In those cases, electro-optic (EO) disparity limits the image quality so that it requires different driving schemes. Therefore, because of the above drawbacks, a transflective LCD with a single cell gap in a single mode configuration needs to be developed for commercial applications. [6, 7]

In this work, we demonstrated two types of transflective LCDs having a single LC mode and a single cell gap. The use of a vertically aligned (VA) or a planarly aligned (PA) configuration combined with a patterned retardation layer allows for brightness-enhancement and/or a single driving scheme.

## 2. The transflective VA LCD

Figure 1 (a) shows the schematic diagram of our transflective VA LCD. The polarizers are parallel to each other. The optic axes of the upper quarter wave plate (QWP) and the easy axis of the LC layer are at

$45^\circ$  and  $-45^\circ$  with respect to the direction of the polarizer, respectively. The patterned retarder has two domains, i.e., the c-plate and the QWP, which are placed in the reflective and the transmissive parts, respectively.

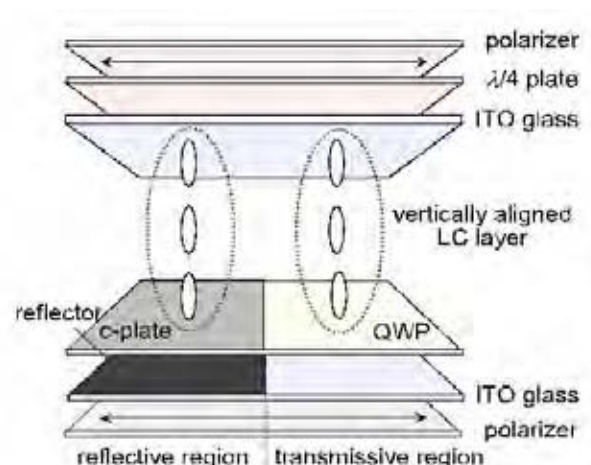


**Figure 1. The schematic diagram of our transflective VA LCD.**

## 2.1 Operating principles

In absence of an applied voltage, the VA LC layer in our transflective LCD has no optical retardation. In the reflective region, a polarization state of linearly polarized input beam from the front polarizer is rotated by  $90^\circ$  through the front QWP, the reflector, and the QWP in sequence. The c-plate does not produce the optical retardation. Therefore, the outgoing light is blocked by the front polarizer.

When an external voltage is applied, the LC layer produces an optical retardation. Above a certain value of the voltage, the LC molecules in the VA layer are reoriented parallel to the substrate, and thus the VA layer behaves as a QWP. The retardation of the front QWP is then optically cancelled through the VA LC layer, eliminating optical retardation. Thus, the outgoing light is transmitted through the front polarizer and a bright state is obtained. In the transmissive region, the polarization state of linearly

polarized input light, from the backlight, through the back polarizer is rotated by  $90^\circ$  from the QWP and the front QWP. The outgoing light is then blocked by the front polarizer in the absence of applied voltage. At a high voltage, the LC is reoriented parallel to the substrate and thus the optical retardation of the QWP is cancelled by the VA LC layer. In this case, the input light undergoes only  $\lambda/4$  optical retardation, and the light is transmitted through the front polarizer.

## 2. 2 Fabrication of a transmissive VA LCD with a retardation plate

For the fabrication of a VA cell, JALS-203 (Japan Synthetic Rubber) was spin-coated onto the indium-tin-oxide (ITO) deposited glass substrate and baked at  $200^\circ\text{C}$  for 1hour. The surface was treated by the rubbing process. Note that an array of metal reflectors was served as an array of mirrors for the reflective part. The polymaleimide based photoreactive polymer was used as an alignment layer. The polymer dissolved in cyclopentanone was coated onto the substrate and baked at  $150^\circ\text{C}$  for 30min. The polarized UV light was irradiated through a photomask for 200sec onto part of the photopolymer. Before applying the polymerizable liquid crystalline (PLC) material [8] coating, the polymer was exposed to UV light without the photomask and the photopolymer was insolubilized in solvent. [9] The PLC, LC-242 (BASF), with photo-initiator, was dissolved in chloroform. The solution was coated onto the UV-treated photopolymer substrate. The LC layer was baked at  $100^\circ\text{C}$  for 1min and polymerized with UV irradiation for 100sec. The fabricated retarder having both homeotropic and planar parts was attached to the VA cell.

We adopted a photopatterned optical compensation layer to achieve the single LC mode in the transmissive LCD. The photopolymer having a photoreactive side chain was used as an alignment layer for PLC monomer. As an alignment layer, this polymer induces an orientational transition of LC from the homeotropic to the planar configuration depending on the UV irradiation. As the photopolymer was irradiated by UV light with an amplitude mask. The PLC monomer, coated onto the treated layer, has homeotropic and planar configurations in unexposed and exposed areas, respectively. The configurations are fixed by the cross-linking reaction. The LC layer has homeotropic and planar domains as shown in Fig. 2 (a) and 2 (b). The homeotropic part

shows the dark state in any direction of the optical axis. In contrast, the planar domain shows dark and bright states depending on the direction of the polarizer. The phase retardation,  $2\pi d\Delta n/\lambda$ , of the retarder was measured using the photoelastic modulation (PEM) technique. [10] Here,  $d$ ,  $\Delta n$ , and  $\lambda$  represent the thickness, the optical anisotropy of the retarder, and the wavelength of the light used, respectively. The measured results are shown in Fig. 2 (c). The maximum phase retardation was about 1.62 in the planar region, which corresponds to  $\lambda/4$  for  $\lambda = 632.8\text{nm}$ . In contrast, the retardation in the homeotropic region was only 0.09.

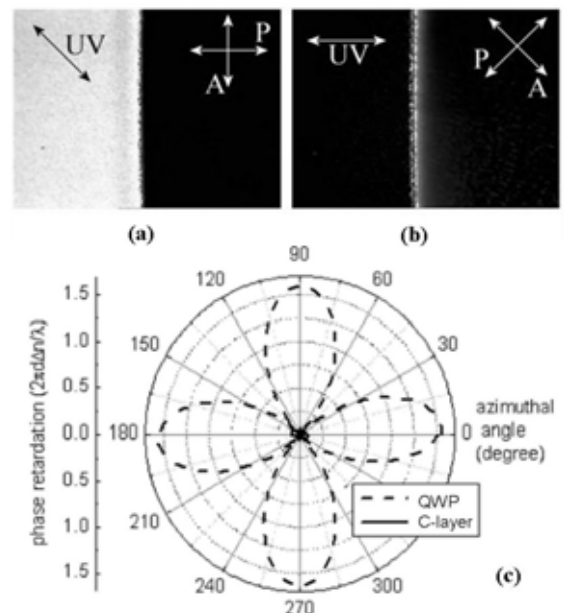


**Figure 2. Microscopic textures of the patterned retarder: (a) and (b) QWP and C-layer observed under crossed polarizers and (c) The phase retardation of the patterned retarder measured by the PEM technique.**

## 2. 3 Electro-optic properties

The experimental and numerical EO results are presented in Fig. 3 by symbols and lines, respectively. The reflectance and transmittance are presented as the ratio of the output intensity to the input intensity. We performed numerical simulations to obtain the EO characteristics of our transmissive LCD using the extended Jones matrix formulation. [11] The profile of the LC director as a function of applied voltage was also simulated based on Oseen's [12] and Frank's [13] continuum theory. The material parameters of LC used for numerical simulations are the elastic

constants  $K_1 = 13.0 \times 10^{-12}$  N and  $K_3 = 15.0 \times 10^{-12}$  N, the ordinary refractive index  $n_o = 1.4620 + 5682/\lambda^2$ , the extraordinary refractive index  $n_e = 1.5525 + 9523/\lambda^2$ . Here,  $\lambda$  is the wavelength of the incident light in 632.8nm. The dielectric anisotropy  $\epsilon_a = -4.9$ , and the rotational viscosity  $\gamma_1 = 0.148$  Pa · sec. The maximum reflectance of our transfective VA LCD was 0.41, which is much higher than the 0.3 for TN [6] and 0.25 for IPS [7]. The brightness of the transmissive region depends on the intensity of the backlight. In contrast, the brightness of the reflective region depends on the ambient light, which cannot be controlled. In this respect, the reflectance is more important for improving the brightness of the transfective LCD itself. Furthermore, the maximum transmittance of our configuration, 0.21, is much lower than the reflectance, while it is similar to the reported value. The difference in brightness between the transmissive and reflective regions due to the different efficiencies can be balanced by adopting a bright backlight or by reducing the size of the reflective region compared with the transmissive region in a pixel. The measured rise and fall times of the response were found to be 2.9 and 0.36 msec, respectively. These fast switching times are due to the small cell gap corresponding to  $\lambda/4$ .

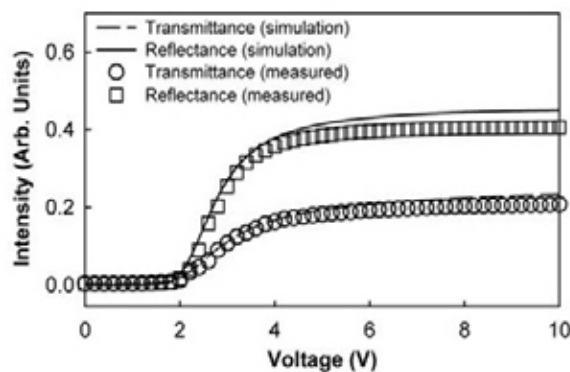


Figure 3. The electro-optic characteristics of a transfective VA LCD.

### 3. The transfective PA LCD

Figure 4 shows the schematic diagram of our transfective PA LCD. In this case, crossed polarizers are used. The LC molecules, whose optical retardation is equal to that of the QWP, are planarly aligned an angle of  $45^\circ$  respect to one of the polarizers in the whole part. In order to compensate the optical path difference, an inner-patterned retarder has two different optic axes, making angles of  $0^\circ$  and  $45^\circ$  with respect to the rear polarizer in the transmissive and

the reflective parts, respectively. In other words, the inner-patterned retarder behaves as an optically dummy layer in the transmissive part and the QWP in the reflective part.

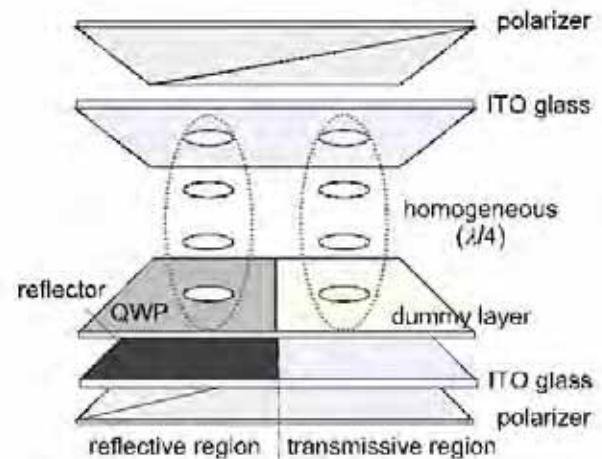


Figure 4. The schematic diagram of transfective PA LCD.

### 3. 1 Operating principles

In the absence of an applied voltage, the LC molecules in our transfective LC cell are uniformly aligned parallel to the substrates. The phase retardation of the LC layer is then equal to  $\lambda/4$ . No polarization rotation of the input light occurs through the inner-patterned retarder in the transmissive part. The input light is converted into a circularly polarized light through the LC layer and thus becomes partially transmitted through the output polarizer. In reflective part, the total retardation through the homogeneously aligned LC layer and the subsequent inner-patterned retarder is  $\lambda/2$ . A linearly polarized input light through the front polarizer, passing twice through the patterned retarder and the LC layer, becomes a linearly polarized light on being reflected from the reflector. Since the polarization direction of the reflected light coincides with the front polarizer, the reflected light is completely transmitted through the front polarizer. Thus, a bright state is obtained.

In the presence of an applied voltage, the LC with a positive dielectric anisotropy becomes to align vertically. In this case, no phase retardation occurs through the LC layer in both the transmissive and reflective parts. In the transmissive part, a linearly polarized light through the rear polarizer is completely blocked by the front polarizer and thus a dark state is obtained. In the reflective part, a linearly

polarized light through the front polarizer undergoes the phase retardation of  $\lambda/4$  on passing through the LC layer and the subsequent patterned retarder. This circularly polarized light becomes a linearly polarized light through the patterned retarder on being bounced back from the reflector. The polarization direction of this reflected light makes an angle of  $90^\circ$  with respect to the front polarizer. Thus, the reflected light is completely blocked by the front polarizer. As a result, a dark state is obtained.

### 3. 2 Fabrication of a transfective PA LCD with an inner-patterned retarder

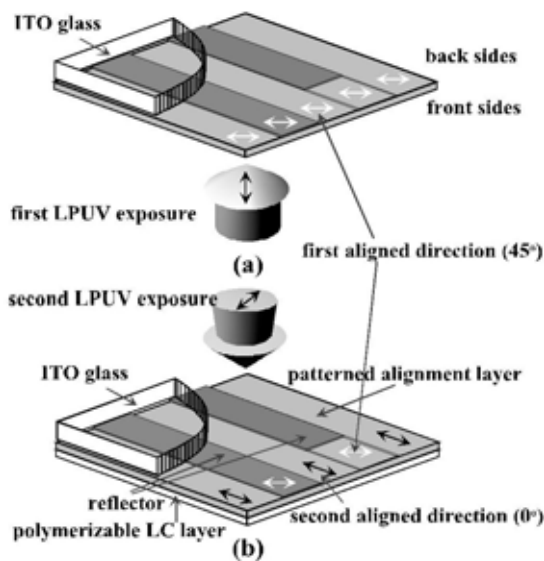


**Figure 5.** The self-masking process by two-step LPUV exposures for fabrication of an inner-patterned retarder.

The transfective LC cell, consisting of a periodically inner-patterned retarder, was fabricated inside the cell through a self-masking process of the photoalignment technique on glass substrates coated with the photopolymer of LGC-M0 (LG Cable Ltd., Korea). In order to create two patterns with an effective retardation of 0 and  $\lambda/4$  in the transmissive and reflective parts, respectively, the photoalignment layer was treated by two successive LPUV exposure steps as shown in Fig. 5. The photoalignment polymer was coated onto the ITO glass substrates with mirrors and baked at  $120^\circ\text{C}$  for 30min. After the first-step LPUV exposure in the whole region, defining one of two easy axes, the second-step LPUV exposure was carried out to define the other easy axis which makes an angle of  $45^\circ$  with respect to the first-defined easy

axis. The second-step LPUV exposure was performed from the outside of the cell not to disturb the first-defined easy axis on the photoalignment layer. [14, 15] Note that an array of metal reflectors was served as an array of mirrors for the reflective part as well as an amplitude photomask for the periodic alignment layer as shown in Fig. 5 (b). A solution of the mixture of photo PLC material, LC-298 (BASF), doped with a photoinitiator was spin-coated on the patterned alignment layers at room temperature. Upon coating, the photo PLC molecules align themselves on the patterned alignment layer. Subsequently, the aligned molecules were exposed to the unpolarized UV light to produce a patterned retardation layer. The inner-patterned retarder in a periodic form, having two different optic axes, makes two angles of  $0^\circ$  and  $45^\circ$  with respect to the rear polarizer in the transmissive and reflective parts, respectively.

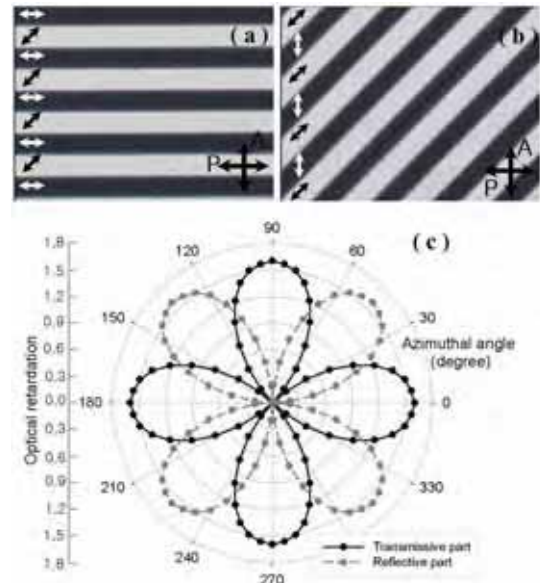


**Figure 6.** Microscopic textures of the patterned retarder: (a) an angle of  $0^\circ$  and (b)  $45^\circ$  between the optic axis of the retarder and the rear polarizer.

Figure 6 shows microscopic textures of the patterned retarder on the ITO glass substrate with no reflectors observed at an angle of  $0^\circ$  and  $45^\circ$  between the optic axis of the retarder and that of one of crossed polarizers under a polarizing optical microscope. As shown in Fig. 6 (a), the patterned retarder shows bright and dark states along the directions of  $45^\circ$  and  $0^\circ$  between the optic axis of the retarder and the rear polarizer. Small black and white arrows coincide with the directions of the first and the second LPUV

exposure, respectively. Fig. 6 (b) shows microscopic textures when the patterned retarder was rotated by an angle of  $45^\circ$  with respect to Fig. 6 (a). In this case, the bright and dark states were reversed. The measured optical retardation of the patterned retarder using the PEM technique was about  $\pi/2$  as shown in Fig. 6 (c).

An array of aluminum reflectors was prepared on the ITO glass substrate. For the homogeneous LC alignment, a photoalignment layer was prepared on the top substrate and over the patterned retarder on the bottom substrate. The easy axis makes an angle of  $45^\circ$  with respect to one of crossed polarizers. The nematic LC material used in this work was MLC-7023 of E. Merck. The extraordinary and ordinary refractive indices of MLC-7023 are  $n_e=1.5254$  and  $n_o=1.4645$  at wavelength of 632.8nm, respectively. The dielectric anisotropy is  $\Delta\epsilon = 7.9$ . The cell thickness was maintained using glass spacers of  $2.4\mu\text{m}$  thick so that the phase retardation of the uniformly aligned LC layer corresponds approximately to  $\lambda/4$  of the wavelength used. A He-Ne laser of 632.8 nm was used as a light source. All the measurements were carried out at room temperature.

### 3. 3 Electro-optic properties

The open circles and rectangles denote the experimental results of the transmittance and the reflectance in Fig. 7, respectively. The solid lines represent the simulation results obtained by the relaxation method in the elastic continuum theory. It is clear that the EO characteristics of the transmissive agree well with those of the reflective parts. This allows for a single driving scheme for our transfective PA LCD.

The transmissive and reflective intensities were measured as a function of the applied voltage from 0 to 10V. The open circles and rectangles denote the experimental results of the transmittance and the reflectance, respectively. The solid lines represent the simulation results obtained by the relaxation method [13] in the elastic continuum theory. [14] As shown in Fig. 7 (a), it is clear that the EO characteristics in the transmissive part follow well those of the reflective part.

Figure 7 (b) shows the measured EO responses of our transfective LC cell to an applied voltage in a square waveform. The open circles and the solid line denote the EO response in the transmissive part and that in

the reflective part, respectively. The EO responses in the two parts are very similar to each other. This is expected from the fact that a single LC mode in both the transmissive and reflective parts as well as a single gap was used in our transfective LC cell. Based on our experimental data of the dynamic EO responses, it is concluded that only a single driving scheme will be needed for our transfective LCD. The measured rising and falling times were found to be 55.7 msec and 10.9 msec, respectively.

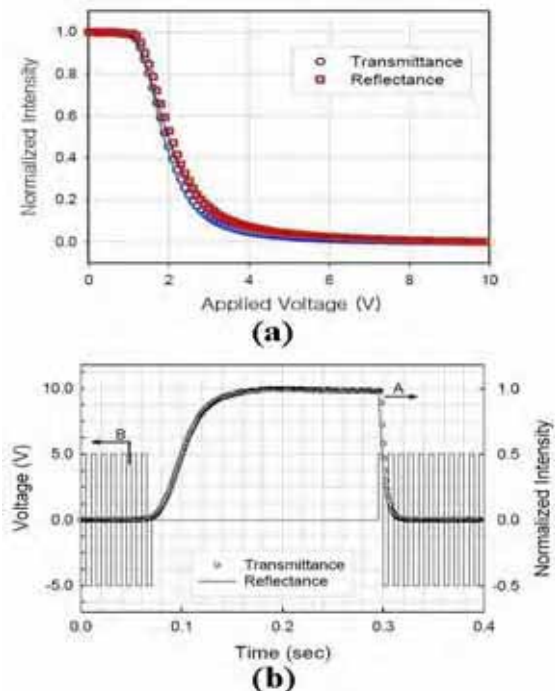


Figure 7. (a) The EO characteristics and (b) the dynamic responses

### 4. Conclusion

We have demonstrated two transfective LCDs having a single cell gap and a single LC mode configuration. In the transfective VA LCD, it was found that the EO characteristics such as the reflectance and the switching times were greatly enhanced. In the transfective PA LCD, the measured EO curves in the transmissive and the reflective parts were found to have common features that allow for a single driving scheme. Moreover, the inner-patterned retarder, fabricated by self-masking photoalignment process, has several advantages such as compactness and no parallax over an external optical film.

### 5. Acknowledgements

This work was supported by Samsung Electronics, AMLCD.

## 6. References

- [1] S. T. Wu and C. S. Wu, *Appl. Phys. Lett.* **68**, 1455 (1996).
- [2] S. H. Lee, K.-H. Park, J. S. Gwag, T.-H. Yoon, and J. C. Kim, *Jpn. J. Appl. Phys.* **42**, 5127 (2003).
- [3] T. B. Jung, J. C. Kim, and S. H. Lee, *Jpn. J. Appl. Phys.* **42**, L464 (2003).
- [4] S. H. Lee, H. W. Do, G.-D. Lee, T.-H. Yoon, and J. C. Kim, *Jpn. J. Appl. Phys.* **42**, L1455 (2003).
- [5] C.-J. Yu, D.-W. Kim, and S.-D. Lee, *Appl. Phys. Lett.* **85**, 5146 (2004).
- [6] J. Kim, D.-W. Kim, C.-J. Yu, and S.-D. Lee, *Jpn. J. Appl. Phys.* **43**, L1369 (2004).
- [7] K.-H. Park, J.-C. Kim, and T.-H. Yoon, *Jpn. J. Appl. Phys.* **43**, 7536 (2004).
- [8] D. J. Broer, J. Lub, and G. N. Mol, *Macromolecules* **26**, 1244 (1993).
- [9] K. Ichimura, Y. Akita, H. Akiyama, K. Kudo and Y. Hayashi, *Macromolecules* **30**, 903 (1997).
- [10] K. W. Hipps and G. A. Crosby, *J. Phys. Chem.* **83**, 555 (1979).
- [11] A. Lien, *Appl. Phys. Lett.* **57**, 2767 (1990).
- [12] C. W. Oseen, *Trans. Faraday Soc.* **29**, 883 (1933).
- [13] F. C. Frank, *Discuss. Faraday Soc.* **25**, 19 (1958).
- [14] W. Gibbons, P. J. Shannon, S. T. Sun, and B. J. Swetlin, *Nature* **351**, 49 (1991).
- [15] M. Schadt, H. Seiberle, and A. Schuster, *Nature* **381**, 212 (1996).